

# Measurement of Shear and Compression Waves During Triaxial Testing

KENNETH C. BALDWIN, PEDRO DE ALBA, ADAM JONES, AND ISMAIL MENGUC

Researchers at the geotechnical laboratory at the University of New Hampshire have developed a technique for measuring shear (*S*) and compression (*P*) wave parameters of triaxial specimens. The triaxial end caps contain *S* and *P* wave transducers. Bender bimorphs are used for *S* waves and thickness expanders are used for *P* waves. These piezoelectric devices are separated from the triaxial specimen by a flexible window, which protects the transducers from failure due to moisture and allows proper coupling of the acoustic energy. Testing to date has focused on two areas. The first is determining the relationship between the acoustic characteristics of sand and liquefaction resistance. Results indicate that material-dependent one-to-one relationships can be established between *S* or *P* wave velocity and liquefaction resistance. Preliminary results from frequency domain measurements related to damping are encouraging as an indicator of sand fabric. The second area is the relationship between shear strength and *S* or *P* wave velocity in clays. Staged tests on marine clays indicate the effects of stress history and plasticity on this relationship.

Acoustic waves are transmitted by soils in ways which are characteristic of the particular fabric and density of the material. Thus, nondestructive, low-amplitude, high-frequency waves can be used to characterize individual soils. Based on this premise, the geomechanics group at the University of New Hampshire (UNH) is in the process of developing techniques for reliably measuring acoustic-wave velocities in the laboratory.

The long-term objective of this work is to develop testing methods to compensate for the effects of disturbance in recovering specimens from the field. Measurements of shear (*S*) and compression (*P*) wave velocity would be made in the field deposit with an acoustic cone or a closely spaced cross-hole setup. Specimens would be recovered and reconsolidated in a triaxial cell (or other apparatus) equipped with an acoustic measurement system until the in situ wave transmission characteristics were restored in the laboratory. Presumably, at that point the specimen would be restored to its in situ condition and could then be subjected to destructive testing along any desired stress path.

Consequently, the fundamental objective of our research effort was to investigate the potential for establishing correlations between large-strain mechanical properties and *S* or *P* wave transmission characteristics for different soils; this in turn has required the development of reliable instrumentation

for generating and receiving acoustic waves in a single triaxial specimen, which is then subjected to large-strain destructive testing under static or dynamic loading.

Presented in this paper is an overview of developments to date, which include the design of small acoustic transducers, capable of generating and receiving *S* and *P* waves and small enough to fit into the end caps of the triaxial cell, as well as the configuration of the required measurement system. Selected results from different studies are presented to illustrate the operation of the system.

## ACOUSTIC TRANSDUCERS

The transducers generate and receive both *S* and *P* waves. Conventional wisdom in the geotechnical community is still that the *P* wave is carried by the water in saturated soils and thus provides no information on the soil fabric below the water table. However, Ishihara (1) pointed out that *P*-wave velocity in saturated soil depends essentially on the bulk modulus of the two-phase material and thus will be affected by the soil structure. The effect of soil fabric on the *P*-wave velocity is smaller than on the *S*-wave velocity; however, precise *P*-wave measurements can give much useful information. The use of *P* waves is most desirable from a practical point of view, because they are easier to generate both in the field and in the laboratory; in the experience of the authors, *P* waves produce a received signal with a leading edge that is easier to identify than that of *S* waves, thus greatly facilitating travel-time measurements.

The acoustic transducers, therefore, had to generate low-strain compression and shear disturbances that did not affect the soil fabric, yet provided sufficient signal strength to determine the acoustic parameters. The acoustic transducers had to provide a means of generating and receiving both *S* and *P* waves both before and during loading of the triaxial specimen under both static and dynamic conditions.

The underwater acoustics and marine geophysics community has a history of using water-tight acoustic transducers. Compression wave transducers have been routinely deployed for water column and sediment acoustic measurements (2-4). Shirley and Anderson (5,6) developed a corehead velocimeter that successfully deployed compression wave transducers in the cutter of a piston corer. They went on to develop an *S*-wave transducer for this device using a piezoelectric bender bimorph.

The bender is constructed from two longitudinally expanding piezoelectric ceramics sandwiched together. When a volt-

K. C. Baldwin, Mechanical Engineering Department, University of New Hampshire, Durham, N.H. 03824. P. de Alba, Civil Engineering Department, University of New Hampshire, Durham, N.H. 03824. A. Jones, Northrup, Devine and Tarbell, Inc., Portland, Maine 04103. I. Menguc, Kingston-Warren Corp., Newfields, N.H. 03856.

age is applied across the bender, one side expands and the other contracts, resulting in a bending motion (Figure 1). As the voltage is varied sinusoidally, the bender produces a sinusoidally varying mechanical displacement. Conversely, a sinusoidal displacement of the bender causes the piezoelectric elements to produce a sinusoidally varying voltage. Thus, benders can both generate and receive *S* waves. The bender element was chosen because its mechanical impedance closely matched that of the sediment (6).

The design concepts embodied in the transducers used in the UNH research originated with the work of Shirley (7) and Baldwin et al. (4). The transducer has a cylindrical body that houses the piezoelectric elements and fits directly into modified triaxial endcaps. The *S*-wave transducers consist of an array of piezoelectric benders mounted in a base plate in a cantilevered fashion. A four-bender array is used to increase the active area in contact with the specimen. This enhances the ability to couple energy into the specimen. The free end of the benders is encapsulated in a flexible polyurethane window (Figure 2). The array generates and receives *S* waves at its resonant frequency. Similar approaches to piezoelectric *S*-wave transducer design for geotechnical testing using benders have been reported by Brunson and Johnson (8), Horn (9), Schultheiss (10), Strachan (11) and Dyvik and Madhus (12). The *S*-wave transducers involved in all these studies, however, used a single bender element that was not encapsulated but projected up to 10 mm into the specimen. This situation can lead to transducer failure due to mechanical loading, causing

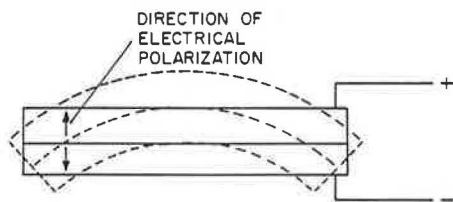


FIGURE 1 Operation of a piezoelectric bender element.

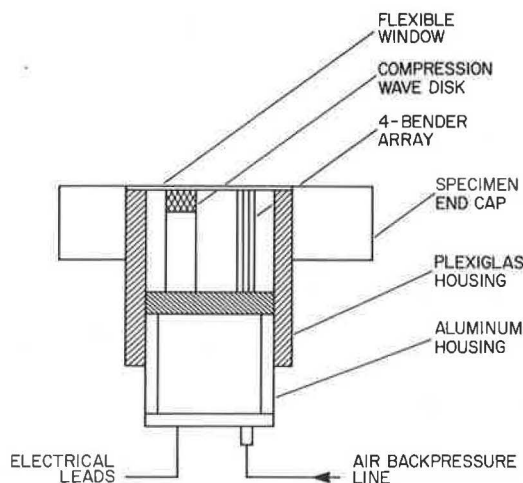


FIGURE 2 End-cap acoustic transducer with *S*- and *P*-wave piezoelectric elements.

undesired bending during insertion as well as short circuits due to moisture effects.

The compression wave transducer uses a thickness-expanding disk. The disk operates at its experimentally determined resonant frequency. The disk is mounted on a pedestal beside the bender array (Figure 2). The free surface of the disk is encapsulated in the flexible window next to the bender array.

The flexible window isolates the piezoelectric elements from the moisture in the soil specimens and provides a surface against which the soil specimens can react and be acoustically coupled to the *S*- and *P*-wave generating elements. The non-wetted side of the window is pressure-compensated to prevent implosion.

The transducer designed shown in Figure 2 was adapted to both 1.4-in.-diameter and 2.8-in.-diameter triaxial specimens. The smaller diameter was used for testing clays in staged triaxial tests, and the larger diameter was used for testing sand in cyclic triaxial liquefaction tests.

## MEASUREMENT SYSTEM

The measurement system was configured to determine propagation times for acoustic pulses across a known specimen length. The acoustic travel time was necessary to determine the *P*- and *S*-wave velocities. The pulse-time delay configuration shown in Figure 3 was used to measure the acoustic travel time.

The pulse generator output was a 10 volt peak to peak, 4 cycle, gated sine wave for both *P*- and *S*-wave generation. The frequency was the only parameter that changed; for *P* waves, the frequency was approximately 140 kHz, and for *S* waves, the frequency was approximately 3 kHz. The signal was used to drive the *S*- or *P*-wave transmitting acoustic transducer and to simultaneously trigger the horizontal sweep on the digital oscilloscope, establishing zero time for the travel-time measurement.

The wave was received by the other transducer, and the signal from this receiver was amplified and band-pass filtered before being displayed on the digital oscilloscope. Band-pass

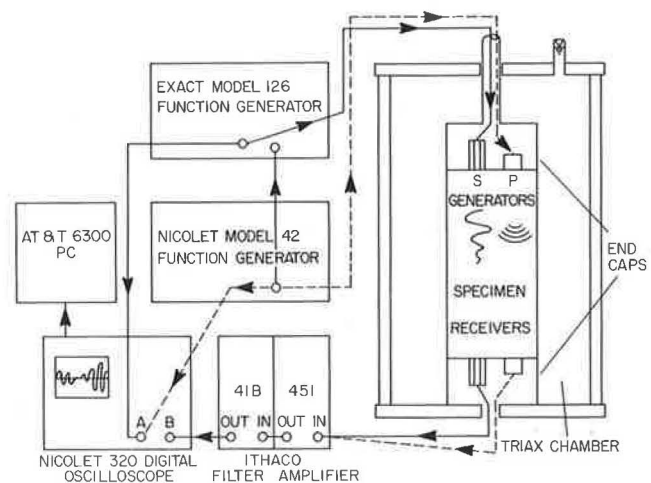


FIGURE 3 Schematic of the acoustic measurement system, transducers, and triaxial chamber.

filtering eliminated noise and passed only those frequencies around the resonant frequency.

The time based on the digital oscilloscope was set to 0.1  $\mu\text{sec}/\text{point}$  for  $P$  waves and 2  $\mu\text{sec}/\text{point}$  for  $S$  waves to permit the appropriate resolution in the time-delay measurements. The time base increments were selected based on the order of magnitude of the expected acoustic travel times.

The digital oscilloscope provided the time base for digitizing signals and making time-delay measurements. Internal software enabled an operator to create a program that stacked the received signals. Stacking is an averaging technique that has been used successfully in geophysics to enhance the leading edge (first arrival) and minimize noise in received signals. This technique was useful in  $S$ -wave velocity measurements and not so critical in  $P$ -wave measurements. After the prescribed number of received signals were stacked, the resulting signal was transferred to a personal computer using the WAVEFORM BASIC software package. The signals were stored on floppy disks for future analysis.

## ACOUSTIC PARAMETERS

Two basic acoustic parameters, wave velocity and quality factor ( $Q$ ), were determined using the data acquired with the transducer and measurement system. The wave velocity is related to the inherent stiffness, and  $Q$  is related to the inherent damping in the soil specimen.

Wave-velocity measurements were readily made from the acoustic time delay defined by the leading edge of the received signal. Both  $P$ - and  $S$ -wave velocities were determined by dividing the specimen length by the acoustic time delay. Of the two types of waves, the  $S$ -wave signal required more careful consideration because the leading edge was not always obvious.

The  $S$ - and  $P$ -wave velocities are important data in characterizing a soil, but alone they do not provide a distinctive characterization. In a study of the dynamic behavior of sands, (13), it was determined that characteristic relationships can be established between  $S$ - or  $P$ -wave velocity and liquefaction resistance, but the range of velocity change that covers the range of sand densities studied was relatively small. It was therefore desirable to extract additional information from the received signals, which would define other characteristic transmission parameters.

$Q$  was borrowed from vibration and electrical circuit analysis. It is a frequency-domain parameter that is related to the center frequency of a signal's spectrum and the frequencies of the half-power points. A graphical representation is shown in Figure 4 (14). The simple expression defining  $Q$  from the spectrum is:

$$Q = \frac{f_{\text{center}}}{f_{\text{upper}} - f_{\text{lower}}}$$

where  $f_{\text{center}}$  is the resonant frequency and  $f_{\text{upper}}$  and  $f_{\text{lower}}$  are the upper and lower half power frequencies, respectively. From vibration theory  $Q$  is defined as follows (2):

$$Q = \frac{1}{2\zeta} \cong \frac{\pi}{\delta}$$

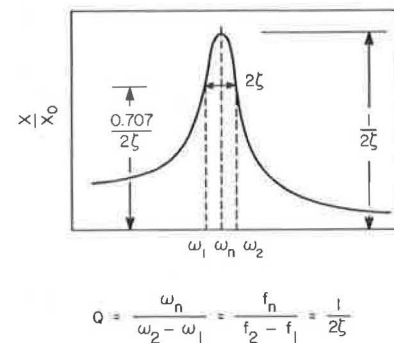


FIGURE 4 Generic spectrum level versus frequency plot indicating the parameters required to determine  $Q$  (14).

where  $\zeta$  is the damping factor in the system and  $\delta$  ( $\leq 0.3$ ) is the logarithmic decrement (14).

There are two approaches to determining  $Q$ , but regardless of the approach used it is imperative that the transducer response be flat in the frequency band of interest. The measurement must display amplitude versus frequency variations that are indicative of the soil response, not the inherent transducer response.

The straightforward way to determine  $Q$  is to drive the transducer with a constant amplitude signal while varying the frequency and noting the changes in received amplitude with frequency. This is done using prescribed frequency increments over a frequency band in which the inherent transducer response is  $\pm 0.5$  dB. This method requires many signals to generate the desired result.

The second approach uses the spectrum calculated from the Fast Fourier Transform (FFT) of the stacked received signals. The FFT is the key to this method. It is important in Fourier analysis to define the maximum and minimum frequencies in the band of interest, but because the signals are band-pass filtered, these are known. Sampling the time series or the stacked acoustic signals to avoid aliasing requires sampling at the Nyquist frequency as a minimum. The period of the sampling frequency or digitizing rate is set by the time base on the digital oscilloscope. The time per point or digitizing rate for  $P$ - and  $S$ -wave data acquisition far exceeds the Nyquist condition.

## PRELIMINARY RESULTS

### Sands

The first application of the measurement system was to investigate whether unique relationships could be defined between liquefaction resistance and  $S$ - or  $P$ -wave velocities in the laboratory (13). For this purpose, cyclic triaxial liquefaction tests were carried out on several different sands; Figures 5 and 6 present results from this study for three uniform materials. Wave velocities,  $S$  and  $P$ , measured immediately before undrained cyclic loading are plotted against the normalized cyclic stress ratio,  $\tau/\sigma'$ , required to cause liquefaction in 10 cycles, where  $\tau$  is the applied cyclic shear stress and  $\sigma'$  is the initial effective confining pressure. These figures indi-

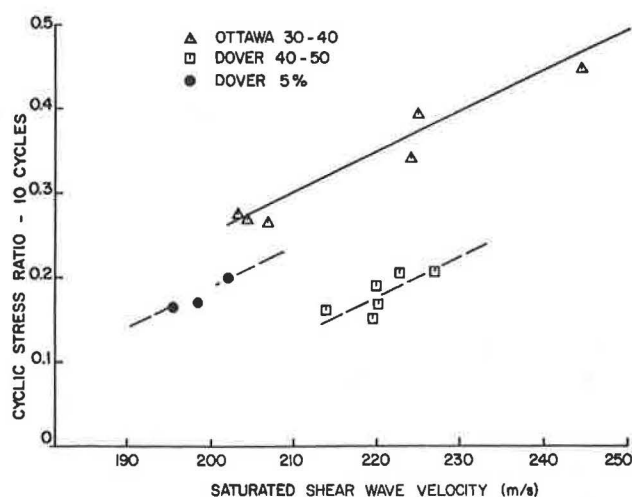


FIGURE 5 *S*-wave velocity versus liquefaction resistance for three uniform sands.

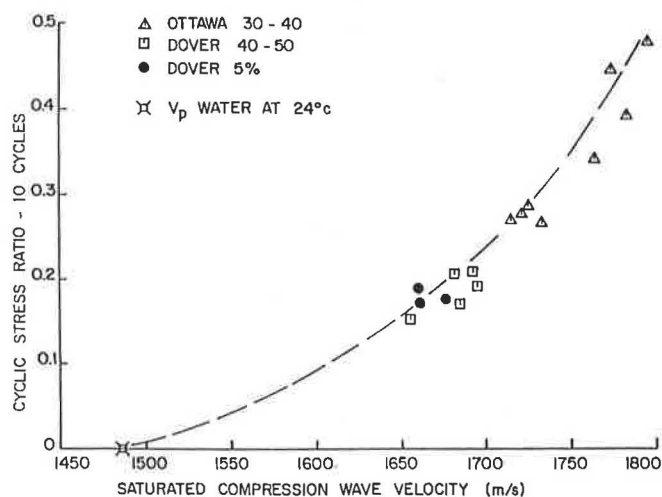


FIGURE 6 *P*-wave velocity versus liquefaction resistance for three uniform sands.

cate that the different materials display characteristic, individual trends, but that the velocity range for the relative density range studied in each material (roughly 55 to 80 percent) is perhaps 5 to 20 percent for *S* waves and 2 to 5 percent for *P* waves. The problem of detecting the leading edge of the acoustic signal also made the technique significantly operator dependent. Consequently, further studies were carried out to reduce operator-dependency in determining the wave velocities and to attempt to define other acoustic wave properties, which could be used to characterize the depositional state of a sand.

In the study of *S*-wave velocity and *Q* in sands by Menguc (15), the *S*-wave signals were amplified 70 dB and filtered in a band between 2.5 and 4.0 kHz. This resulted in an improved signal as seen in Figure 7a and b. The remaining noise on the leading edge was minimized by stacking as shown in Figure 7c. If an infinite number of signals were stacked, then the noise would be zero for the assumed zero-mean process

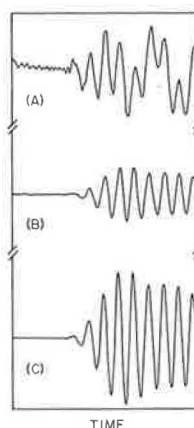


FIGURE 7 Received shear wave signals: (a) unprocessed, (b) filtered, and (c) filtered and stacked.

(16). The "infinite" amount of signals translated to 100 in this case. These improvements, coupled with a fast digital oscilloscope, enhanced the leading edge definition and the velocity determination.

The major concern in this effort was the frequency domain measurements to determine *Q*. The transducers were determined to possess a flat response,  $\pm 1$  dB, in a band from 1.8 to 4.05 kHz. This information helped establish the band width of the filter defined previously. The stacked signals were demeaned and smoothed by applying a cosine taper to the 5 percent of the time series at each end of the series. This minimizes the energy in side lobes when performing an FFT (16).

Fast Fourier transforms were performed on the signals. The resulting amplitude versus frequency plots were normalized relative to the amplitude at the resonant peak. The normalization was

$$\text{dB} = 10 \log \frac{A(f)}{A(f_{\text{res}})}$$

where  $A(f)$  is the amplitude at any frequency in the frequency band, and  $A(f_{\text{res}})$  is the resonant frequency amplitude. The peak was at 0 dB, and all other amplitudes were down (or negative) dB's. This presentation facilitated finding the  $-3$  dB points required to define *Q*. The results for dry-pluviated specimens of a uniform medium sand (Holliston 00) are shown in Figure 8 and summarized in the following table.

Relative Density (percent)	Quality Factor	Log Decrement
53.5	2.25	1.395
66.2	2.47	1.272
70.5	2.57	1.222
72.7	3.00	1.046

Quality factor increases with increasing relative density (*Dr*). This implies that the specimens with high *Dr* have narrow bands,  $(f_u - f_l)$ , and have less damping. This is indicated in the data in the table, where the log decrement is also presented. This result is reinforced by an observation made on the nonnormalized FFT results. The amplitude of the signal at higher *Dr* is higher for the same level of excitation. This indicates that less acoustic energy is dissipated in the speci-



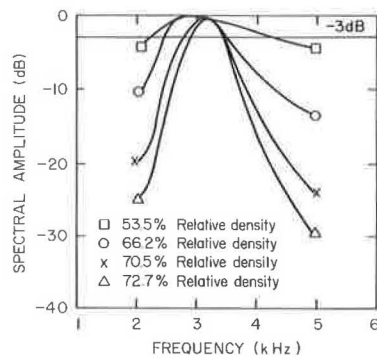


**FIGURE 8** S-wave spectral amplitude (dB) plots for various relative densities.

men, that is, looser fabrics attenuate more readily than denser fabrics.

It should be noted that  $Q$  shows a 33 percent variation over the restricted relative density range studied for this material, a uniform sand with a D50 of 0.5 mm. Thus, these preliminary results suggest that  $Q$  may be a sensitive indicator of soil fabric.

### Clays

A collateral study to those previously described was carried out to determine the relationship between undrained shear strength in marine clays and  $S$  or  $P$ -wave velocity, using a measurement system analogous to that developed for sands (17,18). Preliminary results are reported here for four clay samples, two from the Canadian Beaufort Sea, and two from an exposed marine clay deposit near Portsmouth, New Hampshire.

Staged triaxial tests were performed on each sample following the procedure suggested by Nambiar et al. (19). Further, since the Beaufort material was overconsolidated to a degree that was only approximately known, it was further decided to combine the staged test with the SHANSEP procedure (20), in which samples would first be consolidated to stress levels in excess of the maximum past pressure and then rebounded to obtain known degrees of overconsolidation. This procedure would have the additional important advantage of minimizing the effects of sample disturbance. Analogous tests were carried out in the Portsmouth material, to validate the technique for a deposit with known properties (21).

Staged test results are reported for two Beaufort Sea samples, C3 and D4, and two Portsmouth samples, P1 and P2. The four samples were all consolidated beyond their maximum past pressure into the normally consolidated range, as previously described.

It is interesting to remark that all samples clearly exhibited normalized behavior as defined by Ladd and Foote (20) with the undrained strength ( $S_u$ ) following a relationship for overconsolidated materials of the form

$$\frac{S_u}{\sigma'} = S(\text{OCR})^m$$

where

$\sigma'$  = effective consolidation stress,

$S = S_u/\sigma'$  ratio for normally-consolidated material, and  
OCR = overconsolidation ratio.

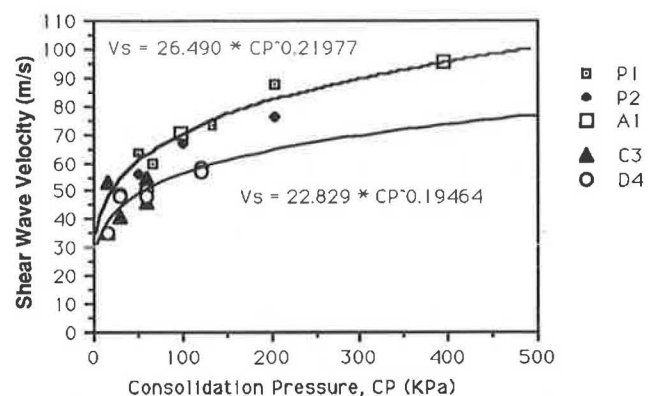
The values of ( $m$ ) varied from about 0.79 for the Beaufort clays to 0.88 for the Portsmouth material. These are within the range reported by Olsen et al. (22) for marine clays. This behavior suggests that the combined stage testing-SHANSEP procedure gives reasonable results. This is further confirmed by the effective-stress friction angle of 21 degrees obtained for the normally consolidated Portsmouth clay, which compares well with that reported by Ladd (21) for this material.

Figure 9, from Baldwin et al. (18), shows the variation in  $S$ -wave velocity ( $V_s$ ) with consolidation stress ( $\sigma'$ ), for all consolidation stages including the shear tests. Two trends can clearly be discerned; one defined by samples P1 and P2, both of which have a plasticity index (PI) of about 15, and the other by the more plastic C3 and D4, which have PI values of 27 and 35 respectively. Curves fitting the general trends indicated are shown in the figure; in both cases,  $V_s$  increase with confining pressure follows an exponential law of the form

$$V_s = K(\sigma')^n$$

where  $n = 0.219$  for the P1 and P2 set; and 0.194 for the C3 and D4 data. These values compare well with  $n = 0.25$ , which was proposed for clays by Hardin and Drnevich (23).

Figure 10 shows the values of  $S$ -wave velocity ( $V_s$ ) obtained immediately before shear testing, plotting against the undrained shear strength ( $S_u$ ) for the various materials. Although each material is seen to behave slightly differently, for purposes of discussion, two general behavior trends may be imposed on the data; one for the more plastic Beaufort materials and the other for the Portsmouth clays. Within each trend, the tests on the normally consolidated material are seen to define a different branch from those on overconsolidated material. The data further suggest that  $V_s$  may be a sensitive indicator of undrained strength change; for example, for the P1 and P2 data, the slope of the normally consolidated branch is about 1.3 kPa/(m/sec), and for C3 and D4 it is approximately 2.8 kPa/(m/sec).



**FIGURE 9** Consolidation pressure versus  $S$ -wave velocity for two marine clays (18).

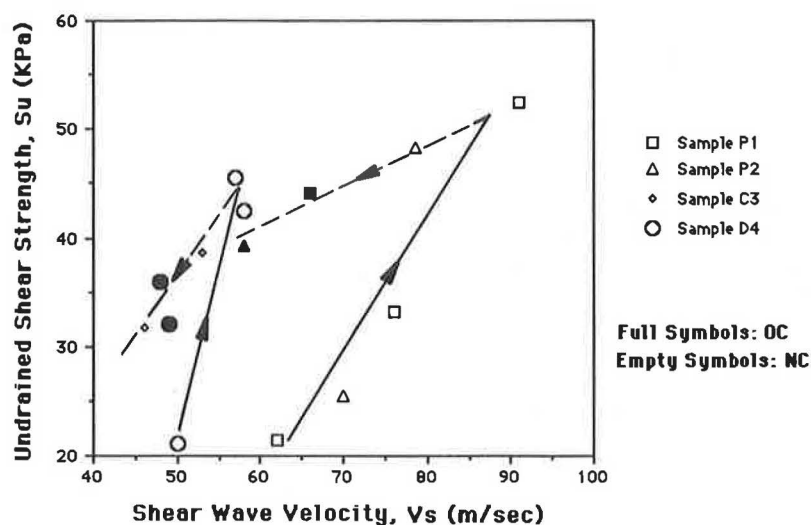


FIGURE 10 S-wave velocity versus undrained shear strength for two marine clays (18).

Figure 11 shows analogous results for  $P$ -wave velocities ( $V_p$ ) versus undrained shear strength for the same materials. In this case, each material defines a unique trend; an interesting feature of this plot is that the normally consolidated branches of the  $V_p$ - $S_u$  relationships have similar slopes.

As for sands,  $V_s$  is seen to be a more sensitive indicator than  $V_p$ ; the slopes of the normally consolidated branches for  $V_p$  in Figure 11 range from about 0.4 to 0.7 kPa/(m/sec), which is roughly half the values obtained for  $V_s$  and, perhaps more importantly, the velocity change over the range of undrained shear strength studied is on the order of 13 to 47 percent of the lowest value measured in the case of  $V_s$ , and only 2 to 3 percent for  $V_p$ .

## SUMMARY

A system has been developed and tested that has the capability of measuring  $P$ - and  $S$ -wave parameters in triaxial spec-

imens, which are then subjected to large-strain destructive testing under static or dynamic loading. It is obvious that definite conclusions cannot be reached on the basis of the limited data available, yet general trends may be noted:

- As expected,  $V_s$  is a more sensitive indicator of large-strain behavior than  $V_p$ ; however, given the relative ease of generating and receiving  $P$  waves in the field and in the laboratory, precise  $V_p$  measurements can be a useful auxiliary indicator.

- For both sands and clays, each soil seems to follow a characteristic relationship between large-strain strength properties and  $S$ - and  $P$ -wave velocity. Consequently, in order to relate  $S$ - or  $P$ -wave measurements in the field to large-strain strength behavior, the characteristic relationship for that particular deposit must be established.

- In clays, stress history is important; the same clay in an overconsolidated state will follow a different  $S_u$ - $V_s$  or  $S_u$ - $V_p$  relationship than in a normally consolidated state. The

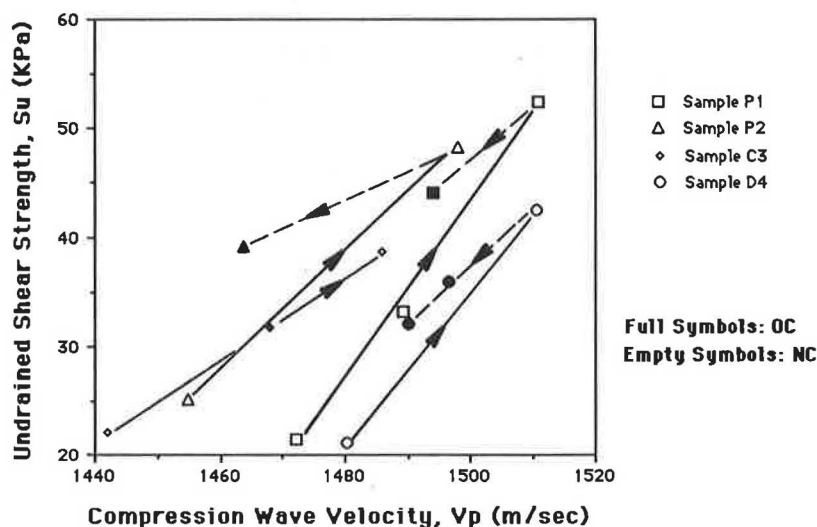


FIGURE 11  $P$ -wave velocity ( $V_p$ ) versus undrained shear strength ( $S_u$ ) for two marine clays.

SHANSEP procedure may be useful in removing disturbance effects and developing the  $S_u$ -wave velocity relationships in clays that exhibit normalized behavior.

• In sands, laboratory testing has shown that unique relationships can be distinguished between liquefaction resistance and  $V_s$  or  $V_p$  for different sands prepared by the same procedure or between series of samples of the same sand prepared by different procedures. The  $Q$ -factor has been seen to be a sensitive indicator of material density for specimens prepared by the same method. All these results suggest that acoustic measurements are sensitive to all factors (including stress history) that affect sand fabric, so that field specimens reconstituted in the laboratory to their field  $V_s$ ,  $V_p$  and  $Q$ -factor values may exhibit large-strain behavior similar to that of the undisturbed field material.

## ACKNOWLEDGMENTS

This work was funded in part by the Geological Survey of Canada, the UNH/UMO Sea Grant Program, the UNH Hubbard Fund, and the UNH Eliot Fund, and for their respective contributions the authors are thankful.

## REFERENCES

1. K. Ishihara. Propagation of Compressional Waves in a Saturated Soil. *Proc., International Symposium on Wave Propagation and Dynamic Properties of Earth Materials*, University of New Mexico Press, Albuquerque, 1968, pp. 195–206.
2. E. L. Hamilton. Sound Velocity and Related Properties of Marine Sediments, North Pacific. *Journal Geophysical Research*, Vol. 75, 1970, pp. 4423–4446.
3. M. L. Silver and C. A. Moore. Shipboard Measurement of Acoustic Velocities in Sediment Cores. Paper OTC 1546. *Proc., 4th Off-shore Technology Conference*, 1972.
4. K. C. Baldwin, B. Celikkol, and A. J. Silva. Marine Sediment Acoustic Measurement System. *Ocean Engineering*, Vol. 8, No. 5, 1981, pp. 481–488.
5. D. J. Shirley and A. L. Anderson. *Compressional Wave Profiliometer for Deep Water Measurements*. Technical Report ARL-TR-74-5. Applied Research Laboratories, University of Texas at Austin, 1974.
6. D. J. Shirley and A. L. Anderson. *Acoustic and Engineering Properties of Sediments*. Report ARL-TR-75-58. Applied Research Laboratory, University of Texas at Austin, 1975.
7. D. J. Shirley. An Improved Shear Wave Transducer. *Journal of the Acoustical Society of America*, Vol. 63, No. 5, 1978, pp. 1643–1645.
8. B. A. Brunson and R. K. Johnson. Laboratory Measurements of Shear Wave Attenuation in Saturated Sand. *Journal of the Acoustical Society of America*, Vol. 68, No. 5, 1980, pp. 1371–1375.
9. I. W. Horn. Some Laboratory Experiments on Shear Wave Propagation in Unconsolidated Sands. *Marine Geotechnology*, Vol. 4, No. 1, 1980, pp. 31–54.
10. P. J. Schultheiss. Simultaneous Measurement of P and S Wave Velocities During Conventional Laboratory Testing Procedures. *Marine Geotechnology*, Vol. 4, No. 4, 1981, pp. 343–367.
11. P. Strachan. An Investigation of the Correlation Between Geophysical and Dynamic Properties of Sand. *Proc., Oceans 81, Vol. 1, Publication No. 81CH1685-7 of the Institute of Electrical and Electronic Engineers Council on Ocean Engineering*, Boston, Mass., 1981, pp. 399–403.
12. R. Dyvik and C. Madhus. Lab Measurements of Gmax Using Bender Elements. *Advances in the Art of Testing Soils Under Cyclic Conditions*, ASCE, 1985.
13. P. de Alba, K. C. Baldwin, V. Janoo, G. Roe, and B. Celikkol. Elastic-Wave Velocities and Liquefaction Potential. *Geotechnical Testing Journal*, GTJODJ, Vol. 7, No. 2, ASTM 1984, pp. 77–87.
14. W. Thomson. *Theory of Vibration with Applications*, Prentice-Hall, Inc., 1981.
15. I. Menguc. A Study of the Experimental Evaluation of Shear Wave Characteristics in Saturated Sands. M.S. thesis. University of New Hampshire, Durham, 1986.
16. J. S. Bendat and A. G. Piersol. *Random Data Analysis and Measurement Procedures*. Wiley-Interscience, 1971.
17. A. Jones. Measurements of Acoustic Properties of Marine Clays in Triaxial Tests, Project paper for the M.S. University of New Hampshire, Durham, 1989.
18. K. C. Baldwin, P. de Alba, and A. N. Jones. Relationship Between Acoustic and Mechanical Properties of Two Marine Clays. *Shear Waves in Marine Sediments* (in press), 1991.
19. M. R. M. Nambiar, G. V. Rao, and S. K. Gulhati. Multistage Triaxial Testing: A Rational Procedure. *Strength Testing of Marine Sediments: Laboratory and In-Situ Measurements* (R. C. Chaney and K. R. Demars, eds.). ASTM STP 883. Philadelphia, Pa., 1985, pp. 274–293.
20. C. C. Ladd and R. Foote. New Design Procedures for Stability of Soft Clays. *Journal of the Geotechnical Engineering Division*, ASCE, Vol. 100, No. GT7, 1974, pp. 763–786.
21. C. C. Ladd. Test Embankment on Sensitive Clay. *ASCE, SMFD Specialty Conference on Performance of Earth and Earth Supported Structures*, Purdue University, 1972, pp. 101–129.
22. H. W. Olsen, T. L. Rice, P. W. Mayne, and R. D. Singh. Piston Core Properties and Disturbance Effects. *Journal of the Soil Mechanics and Foundation Division*, ASCE, Vol. 112, No. 6, 1986, pp. 608–625.
23. B. O. Hardin and V. P. Drnevich. Shear Modulus and Damping in Soils: Measurement and Parameter Effects. *Journal of the Soil Mechanics and Foundation Division*, ASCE, Vol. 98, No. SM6, 1972, pp. 603–624.

Publication of this paper sponsored by Committee on Soils and Rock Instrumentation.